Published in final edited form as:
J Cell Sci. 2013 May 1; 126(0 9): 2092–2101. doi:10.1242/jcs.jcs124537.

Stable incorporation versus dynamic exchange of β subunits in a native Ca^{2+} channel complex

Marta Campiglio, **Valentina Di Biase**[*], **Petronel Tuluc**[‡], and **Bernhard E. Flucher**[§]
Department of Physiology and Medical Physics, Medical University Innsbruck, A-6020 Innsbruck, Austria

Summary

Voltage-gated Ca^{2+} channels are multi-subunit membrane proteins that transduce depolarization into cellular functions such as excitation–contraction coupling in muscle or neurotransmitter release in neurons. The auxiliary β subunits function in membrane targeting of the channel and modulation of its gating properties. However, whether β subunits can reversibly interact with, and thus differentially modulate, channels in the membrane is still unresolved. In the present study we applied fluorescence recovery after photobleaching (FRAP) of GFP-tagged α_1 and β subunits expressed in dysgenic myotubes to study the relative dynamics of these Ca^{2+} channel subunits for the first time in a native functional signaling complex. Identical fluorescence recovery rates of both subunits indicate stable interactions, distinct recovery rates indicate dynamic interactions. Whereas the skeletal muscle β_{1a} isoform formed stable complexes with $Ca_V1.1$ and $Ca_V1.2$, the non-skeletal muscle β_{2a} and β_{4b} isoforms dynamically interacted with both α_1 subunits. Neither replacing the I–II loop of $Ca_V1.1$ with that of $Ca_V2.1$, nor deletions in the proximal I–II loop, known to change the orientation of β relative to the α_1 subunit, altered the specific dynamic properties of the β subunits. In contrast, a single residue substitution in the α interaction pocket of β_{1a}M293A increased the FRAP rate threefold. Taken together, these findings indicate that in skeletal muscle triads the homologous β_{1a} subunit forms a stable complex, whereas the heterologous β_{2a} and β_{4b} subunits form dynamic complexes with the Ca^{2+} channel. The distinct binding properties are not determined by differences in the I–II loop sequences of the α_1 subunits, but are intrinsic properties of the β subunit isoforms.

Keywords

β subunit; Ca^{2+} channels; $Ca_V1.1$; FRAP; Skeletal muscle

[§]Author for correspondence (bernhard.e.flucher@i-med.ac.at).
[*]Present address: Institute of Biophysics, Medical University of Graz, A-8010 Graz, Austria
[‡]Present address: Department of Pharmacology and Toxicology, University of Innsbruck, A-6020 Innsbruck, Austria
Author contributions: M.C., V.D.B. and B.E.F. designed research; M.C. performed research; M.C., V.D.B. and P.T. analyzed data; B.E.F. and M.C. wrote the paper.

Introduction

Voltage-gated Ca^{2+} channels are expressed in all excitable tissues where, in response to membrane depolarization, they control a variety of cell functions like contraction of muscles, secretion in endocrine cells and neurons, or gene regulation. Functional Ca^{2+} channels consist of one α_1 subunit and at least one extracellular $\alpha_2\delta$ and a cytoplasmic β subunit. The α_1 subunit forms the voltage-sensor and the channel pore, whereas the auxiliary $\alpha_2\delta$ and β subunits function in membrane targeting and modulation of gating and current properties. Multiple genes and splice variants of each subunit give rise to a considerable number of possible subunit combinations with distinct expression and distribution patterns, biophysical and pharmacological properties. A given α_1 subunit can combine with different $\alpha_2\delta$ and β subunits in different cell types and at different developmental stages. However, it is still a matter of debate whether the auxiliary subunits can also dynamically exchange in native Ca^{2+} channel complexes and thus differentially modulate pre-existing channels in the membrane (Buraei and Yang, 2010).

In skeletal muscle the Ca_V 1.1 voltage-gated Ca^{2+} channel forms a signaling complex with the Ca^{2+} release channel (type 1 ryanodine receptor, RyR1) in the triad junctions between the transverse (T−) tubules and the sarcoplasmic reticulum (SR). Upon depolarization $Ca_V1.1$ activates the opening of the RyR1 and the resulting Ca^{2+} release from the SR then triggers excitation–contraction (EC−) coupling. This interaction of $Ca_V1.1$ and RyR1 depends on their physical interaction by the cytoplasmic loop between repeats II and III of the α_{1S} subunit (Grabner et al., 1999) and probably also by the β_{1a} subunit (Cheng et al., 2005). A highly regular spatial organization of groups of four $Ca_V1.1$s (termed tetrads) opposite the RyR1 is the structural correlate of this direct mode of EC coupling in skeletal muscle (Franzini-Armstrong et al., 1998). Whether the putative physical interactions between the $Ca_V1.1$ α_{1S} and β_{1a} subunits and the RyR1, which are essential for tetrad formation and direct EC coupling, also result in an increased stability of the Ca^{2+} channel signaling complex in skeletal muscle is hitherto unknown.

Here we applied fluorescence recovery after photobleaching (FRAP) analysis in dysgenic myotubes reconstituted with GFP-tagged Ca_V1 α_1 and β subunits to study the dynamics or stability of Ca^{2+} channel subunits in the native environment of the triad junction. The skeletal muscle β_{1a} subunit was stably associated with the α_{1S} subunit. In contrast, higher fluorescence recovery rates of non-skeletal muscle β subunits compared with those of the skeletal muscle α_{1S} and β_{1a} subunits, for the first time demonstrate in a differentiated mammalian cell system that the auxiliary β subunits of the voltage-gated Ca^{2+} channel can dynamically exchange with the channel complex on a minute time scale. An affinity-reducing mutation in the β_{1a} subunit increased the dynamic exchange of the β subunit within the channel clusters, whereas changing the sequence or orientation of the $Ca_V1.1$ I–II loop did not affect the stability of the Ca^{2+} channel complex. Thus, intrinsic properties of the β subunits determine whether they form stable (β_{1a}) or dynamic (β_{2a}, β_{4b}) complexes with α_1 subunits.

Results

$Ca_V1.1$ and $Ca_V1.2$ α_1 subunits are both stably incorporated in triad junctions of dysgenic myotubes

In order to determine the dynamics of $Ca_V1.1$ α_{1S} subunits in skeletal muscle triads and to establish a baseline for subsequent comparison with the dynamics of β subunits, we applied FRAP recordings in dysgenic myotubes reconstituted with GFP-tagged α_{1S} subunits (GFP-α_{1S}). Imaging of living myotubes using a laser scanning microscope (Fig. 1A) showed that, consistent with our previous immunofluorescence labeling experiments (Flucher et al., 2000a), GFP-α_{1S} is localized in discrete clusters in the plane of the plasma membrane. These clusters colocalized with the RyR1 (supplementary material Fig. S1A) and thus resemble developing triad junctions between the plasma membrane and the SR. Moreover, extensive previous and ongoing functional studies demonstrated that these junctions are physiologically equivalent to Ca^{2+} release units, i.e. triad junctions, in mature skeletal muscle fibers (Kasielke et al., 2003; Obermair et al., 2005).

For the FRAP analysis we bleached the fluorescence of the GFP-tagged channel subunit by applying high intensity laser power to a circular region of interest (ROI) containing several fluorescent clusters. Then the recovery of fluorescence in the clusters was observed at high sampling rate for 90 s followed by recording at reduced sampling rate to limit photobleaching for up to 6 min. Fluorescence outside the clusters in the bleached ROI was subtracted from the signal originating from clusters to specifically analyze the Ca_V1 channel dynamics within the junctional signaling complex. The magnified images of a representative experiment (Fig. 1A) show the degree of bleaching and recovery immediately after, 75 s and 6 min after bleaching. The trace below shows the corresponding example recording of the normalized and bleaching-corrected fluorescence intensity in the bleached clusters. As expected for a channel tightly incorporated into a signaling complex, the fluorescence of GFP-α_{1S} showed little to no recovery within the 6-minute observation time. During the initial recording phase the sample was stable enough to allow fitting and calculation of mean recovery curves (Fig. 1A). The value of the fitted curve at 75 s after bleaching was chosen to calculate the fractional fluorescence recovery (R_{75}) used for descriptive and comparative statistics. R_{75} of GFP-α_{1S} was 16.2±2.8% of the pre-bleaching intensity.

The cardiac channel $Ca_V1.2$ also clusters in triad junctions (supplementary material Fig. S1B) but does not physically interact with the RyR1, as evidenced by the lack of tetrad formation and Ca^{2+} current-independent EC coupling (Takekura et al., 2004; Tuluc et al., 2007). Nevertheless, FRAP analysis of GFP-α_{1C} revealed that this channel was just as stably incorporated in the triads as the skeletal muscle GFP-α_{1S} (Fig. 1B). The mean recovery curves of the two α_1 subunits were virtually indistinguishable and R_{75} for GFP-α_{1C} was 16.4±2.9%, which was not significantly different from that of GFP-α_{1S}. Together these results indicate that both Ca_V1 Ca^{2+} channels are stably incorporated into the EC coupling signaling apparatus of skeletal myotubes, and that the distinct coupling mechanisms of $Ca_V1.1$ and $Ca_V1.2$ to the RyR1 are not reflected by differences in their stability of incorporation.

Skeletal muscle β_{1a} subunits form stable complexes with $Ca_V1.1$ in the triad junctions

Next we studied the dynamics of the Ca_V β subunit by coexpressing untagged α_{1S} ($Ca_V1.1$) with GFP-tagged skeletal muscle β_{1a} subunit (β_{1a}-GFP). We hypothesized that β_{1a}-GFP would show the same degree of fluorescence recovery as GFP-α_{1S}, if both subunits form a stable channel complex. On the other hand, higher FRAP rates of β in the clusters compared with that of the α_1 subunit would indicate a dynamic exchange of the β subunits with the channel.

When expressed without an α_1 subunit in dysgenic myotubes, β_{1a}-GFP revealed a diffuse cytoplasmic distribution pattern (Fig. 2A), consistent with previous immunofluorescence studies (Neuhuber et al., 1998a). After photobleaching the fluorescence in the ROI recovered almost instantaneously and R_{75} was 100.8±0.8% (Fig. 2A). This high recovery rate was similar to that of soluble eGFP expressed in dysgenic myotubes (supplementary material Fig. S2A), suggesting that in the absence of an α_1 subunit, β_{1a}-GFP is freely diffusible within the cytoplasm and has no relevant binding sites in the triads. In contrast, when coexpressed with α_{1S}, β_{1a}-GFP showed a clustered distribution pattern (supplementary material Fig. S3A). This demonstrates that recombinant β_{1a}-GFP can readily compete with endogenous β_{1a} for its binding sites in the junctional Ca^{2+} channel complex. After photobleaching β_{1a}-GFP coexpressed with α_{1S} showed little to no recovery within 6 min (Fig. 2B). The mean recovery curve during the first 75 s was practically identical to that of GFP-α_{1S} and the R_{75} of 16.2±2.8% was not significantly different from that of GFP-α_{1S} (Fig. 2B′). The observation that in triads the fluorescence of GFP-tagged β_{1a} and GFP-α_{1S} subunits recover at the same rates indicates that the two skeletal muscle Ca^{2+} channel subunits form a stable complex with one another and move or turn over together. But is this also the case for heterologous β subunits?

Heterologous β subunits dynamically exchange with the $Ca_V1.1$ channel complex in the triad on a minute time scale

The β_{2a} subunit is distinct from all other β subunits in that it is palmitoylated and thus associates with the plasma membrane even in the absence of an α_1 subunit (Chien et al., 1996). Accordingly, β_{2a}-eGFP expressed without an α_1 subunit in dysgenic myotubes showed strong membrane localization (see below, Fig. 3A). When photobleached, its fluorescence recovered quickly (R_{75} 79.9±4.1%), but not at the same rapid rate as the cytoplasmic β_{1a} subunits. The recovery rate of β_{2a}-eGFP was similar to that of GAP-GFP, another palmitoylated GFP probe (supplementary material Fig. S2C). When coexpressed with α_{1S}, β_{2a}-eGFP redistributed into clusters (supplementary material Fig. S3B), indicating that it too could successfully compete with endogenous β_{1a} subunits for binding sites in the Ca^{2+} channel complex. However, different from β_{1a}-GFP its fluorescent clusters substantially recovered within the first minutes after bleaching. Its R_{75} was 39.9±3.5% and thus 2.5×higher than that of GFP-α_{1S} or β_{1a}-GFP (Fig. 2C,C′,E).

This increased mobility could either reflect an increased exchange of β_{2a} with $Ca_V1.1$ channels or an increased mobility of the entire channel complex due to the association of a heterologous β subunit. To distinguish between these two possibilities we analyzed the recovery of fluorescence of GFP-α_{1S} when coexpressed with the heterologous β_{2a} subunit.

Interestingly, also under these conditions GFP-α_{1S} clusters did not recover (supplementary material Fig. S4) and the R_{75} of GFP-α_{1S} coexpressed with β_{2a} (13.3±3.7%) was not significantly different from that of GFP-α_{1S} coexpressed with β_{1a} (R_{75} 16.2±2.8%) (Fig. 3D). Thus, the substantial mobility of the β_{2a} subunit in clusters of stable $Ca_V1.1$ α_{1S} subunits clearly indicates that β_{2a}-eGFP can dynamically exchange with the Ca^{2+} channel complex in skeletal muscle triads.

To clarify whether this reduced stability of β_{2a}-eGFP in Ca^{2+} channel complexes is a general property of heterologous β subunits or is related to the fact that β_{2a} is a palmitoylated membrane protein, we repeated the experiment with a non-palmitoylated heterologous β subunit, β_{4b}-eGFP. Its diffuse distribution when expressed without an α_1 subunit, and its rapid recovery in FRAP experiments similar to that of soluble eGFP verified that β_{4b}-eGFP is cytoplasmic like β_{1a}-GFP (supplementary material Fig. S2B). Similar to the other β isoforms and consistent with previous findings (Subramanyam et al., 2009), β_{4b} also partitioned in the triadic Ca^{2+} channel complex when coexpressed with α_{1S} (supplementary material Fig. S3C). However, different from β_{1a}-GFP, β_{4b}-eGFP showed an elevated recovery rate after photobleaching (Fig. 2D; Fig. 2D′). Its R_{75} of 35.5±2.4% was about twice as high and significantly different from that of GFP-α_{1S} or that of the homologous GFP-tagged β_{1a} subunits (Fig. 2E). This result indicates that, like the heterologous β_{2a}-eGFP, also the heterologous β_{4b} subunit dynamically exchanges with the Ca^{2+} channel complex in the triad.

In order to examine whether the difference in the stability/dynamics of the homologous β_{1a} compared with the heterologous β_{2a}-eGFP and β_{4b}-eGFP subunits is also reflected in their ability to compete with the endogenous β_{1a} for incorporation in the Ca^{2+} channel complex, we quantified the degree of co-clustering of the three β subunits with α_{1S}. Myotubes co-transfected with α_{1S} plus either β_{1a}-GFP, β_{2a}-eGFP, or β_{4b}-eGFP were immunolabeled and analyzed for colocalization of the β subunits with α_{1S} clusters. Whereas clusters of β_{1a}-GFP and α_{1S} were colocalized in practically all myotubes expressing α_{1S} clusters (96.6±1.9%), co-clustering of β_{2a}-eGFP and β_{4b}-eGFP with α_{1S} was only observed in about half of the myotubes (56.6±1.9% and 44.4±2.9%, respectively) (Fig. 2F; supplementary material Fig. S3A–C). Thus, increased dynamic exchange of the heterologous β_{2a} and β_{4b} subunits in the junctional Ca^{2+} channel complex correlates with their decreased ability to form identifiable complexes with α_{1S} subunits in the developing triad junctions.

The stability of the β_{1a} subunits in the triad Ca^{2+} channel complex is independent of the Ca_V1 α_1 subunit isoform

Since the homologous β_{1a}-GFP formed a stable complex with the skeletal muscle α_{1S} subunit, whereas the heterologous β_{2a}-eGFP and β_{4b}-eGFP subunits formed dynamic complexes, we reasoned that these association characteristics might be altered or even reversed when the β subunits are coexpressed with the non-skeletal muscle $Ca_V1.2$ α_{1C} subunit. On coexpression with α_{1C}, β_{2a}-eGFP also became redistributed into triad clusters and its fluorescence recovery rate was dramatically reduced compared with that of β_{2a}-eGFP expressed alone (Fig. 3A,B). However, the mean R_{75} of 42.5±4.9% of β_{2a}-eGFP combined with its homologous α_{1C} subunit partner was still significantly higher than that of the GFP-

α_{1C} subunit itself and was not significantly different from β_{2a}-eGFP's recovery rate when combined with α_{1S} (Fig. 3D). Thus, also when coexpressed with its native channel partner α_{1C}, the non-skeletal muscle β_{2a}-eGFP subunit formed a dynamic complex with the Ca^{2+} channel in the skeletal muscle triad. Therefore, the dynamic association of β_{2a} with Ca_V1 channels is an intrinsic property of the β subunit that does not depend on differences between the $Ca_V1.1$ and $Ca_V1.2$ α_1 subunits.

By itself this finding does, however, not exclude the possibility that the higher stability of the β_{1a}-GFP subunit observed when coexpressed with $Ca_V1.1$ α_{1S} may result from its specific association with its homologous skeletal muscle channel partner. Alternatively, the high stability might result from additional specific binding sites of this β isoform in the triad, including those suggested specifically between β_{1a} and the RyR1. If so, its fluorescence recovery rate after photobleaching would be expected to increase when coexpressed with the heterologous $Ca_V1.2$ α_{1C} subunit, which does not directly interact with RyR1. However this was not the case. When expressed together with α_{1C}, β_{1a}-GFP clusters showed little recovery within 6 min and the R_{75} of 23.6±3.6% was only slightly higher but not significantly different from those of GFP-α_{1C} or of β_{1a}-GFP coexpressed with GFP-α_{1S} (Fig. 3C,D). Together these results suggest that the high stability of β_{1a} in the triad Ca^{2+} channel complex does neither depend on its homologous association with the skeletal muscle $Ca_V1.1$ α_{1S} subunit nor on its isoform-specific interactions with the RyR1 (Cheng et al., 2005; Grabner et al., 1999). Instead it seems to reflect an intrinsically strong binding of β_{1a} to Ca_V1 channels either by a higher affinity to the AID site or by additional secondary binding sites.

Mutations of the $Ca_V1.1$ I–II loop and the β_{1a} subunit differentially affect triad targeting and the stability of the β_{1a} subunit in the Ca^{2+} channel complex

One possible mechanism explaining the differences in the stability/dynamics of distinct α_1–β subunit pairs could be sequence differences within the primary protein–protein interaction site, the α_1 subunit I–II loop containing the AID and the corresponding α binding pocket in the beta subunit. To examine the importance of the specific I–II loop sequence of L-type (Ca_V1) Ca^{2+} channels for the high stability of complexes with β_{1a} we generated an $Ca_V1.1$ chimera containing the I–II loop of the $Ca_V2.1$ α_{1A} subunit (α_{1S}I–IIA) (Fig. 4A). The chimeric approach was necessary because α_{1A} heterologously expressed in dysgenic myotubes is not targeted into triads (Flucher et al., 2000b). In contrast, the α_{1S}I–IIA chimera was targeted into triads, albeit at a substantially reduced rate. Whereas 89±2.1% of myotubes expressing wild type α_{1S} showed a clustered distribution pattern, clustering was achieved in only 32.6±3.0% of α_{1S}I–IIA expressing myotubes (Fig. 4B; supplementary material Fig. S1C,D). This was not accompanied by a reduction of the whole-cell Ca^{2+} currents density (α_{1S} −2.8±0.8 pA/pF; α_{1S}I–IIA −4.4±1.0 pA/pF) indicating that replacing the I–II loop of α_{1S} with that of α_{1A} specifically perturbed triad targeting but not functional membrane expression of this chimera.

Analysis of β association with this construct using double immunofluorescence labeling demonstrated that only 50.6±11.4% of the myotubes forming α_{1S}I–IIA clusters showed colocalized β_{1a}-GFP clusters. By comparison, β_{1a}-GFP was co-clustered in almost all

(96.6±1.9%) myotubes expressing wild type α_{1S} (Fig. 4C; supplementary material Fig. S3A,D). Surprisingly, even though the total number of myotubes with α_{1S}I–IIA/β_{1a}-GFP co-clusters was greatly reduced compared with that of wild type α_{1S}/β_{1a}-GFP, fluorescence recovery after photobleaching was not increased (Fig. 4D). For α_{1S}I–IIA/β_{1a}-GFP, R_{75} was 20.5±3.8%, which is not significantly different from that of β_{1a}-GFP coexpressed with α_{1S} (19.9±4.3%) (Fig. 4G). These similar recovery rates are consistent with the published results of an isothermal titration calorimetry study showing that $Ca_V1.1$ and $Ca_V2.1$ AID peptides bind β subunits with similar affinities in the low nanomolar range (Van Petegem et al., 2008). Apparently, replacing the I–II loop with that of α_{1A} compromises triad targeting and the formation of stable Ca^{2+} channel complexes, but not their stability once they have been formed.

If sequence differences in the primary interaction domain, the I–II loop, do not explain the differential stability/dynamics of distinct α_1–β subunit pairs, isoform-specific secondary interactions within the signaling complex may be involved. In order to displace β from such putative secondary interaction sites without affecting the primary interaction with the AID, we deleted one, two, or three amino acids from the proximal I–II loop of $Ca_V1.1$. This sequence forms a rigid connection between the IS6 transmembrane helix and the AID (Van Petegem et al., 2004). Therefore the three deletions are expected to rotate or tilt the I–II loop relative to the channel. Analogous deletions in $Ca_V2.2$ have previously been shown to displace secondary α_1–β interactions and thus alter β-dependent modulation of N-type ($Ca_V2.2$) Ca^{2+} currents without changing the integrity of the AID (Mitra-Ganguli et al., 2009; Vitko et al., 2008). Immunofluorescence labeling showed that expression and clustering of the three deletion constructs were not significantly different from wild type α_{1S} (α_{1S}del1 85±8.2%, α_{1S}del2 84.7±4.8%, α_{1S}del3 91.3±2.3%, compared with α_{1S} 89±2.1%) (Fig. 4B; supplementary material Fig. S1E–G). More importantly, also co-clustering of the β_{1a} subunit with the three deletion constructs was not altered (α_{1S}del1 98.9±1.1%, α_{1S}del2 95±1.4%, α_{1S}del3 98.3±1.4%, compared with α_{1S} 96.6±1.9%) (Fig. 4C; supplementary material Fig. S3E–G), indicating that changing the orientation of the I–II loop and the β subunit relative to the channel does not affect the formation of channel complexes. Finally, FRAP analysis revealed that deletion of one or more amino acids did not reduce the stability of the complex with β_{1a}-GFP (Fig. 4E; supplementary material Fig. S5). R_{75} was 20.9±3.2% for α_{1S}del1, 19.9±3.8% for α_{1S}del2 and 22.8±4.6% for α_{1S}del3 and thus in no case significantly different from that of β_{1a}-GFP coexpressed with wild type α_{1S} (Fig. 4G). Together these experiments show that neither changing the I–II loop sequence nor the orientation of the I–II loop relative to the channel reduced the stability of the β_{1a}-GFP/α_{1S} complex in skeletal muscle triads.

Therefore we turned our attention to the β subunit and examined the importance of the α binding pocket by introducing a single residue exchange in β_{1a} (M293A). In previous biochemical and functional studies the equivalent mutation in β_{2a} has been shown to reduce the affinity of binding to AID peptides, but still allowed functional modulation of the channel, when coexpressed in oocytes at sufficiently high local concentrations (Maltez et al., 2005; Opatowsky et al., 2004; Van Petegem et al., 2008). Therefore we expected that on coexpression with α_{1S} in dysgenic myotubes β_{1a}M293A-GFP might still co-assemble with the channel in triads, and thus permit FRAP analysis. Indeed β_{1a}M293A-GFP co-clustered

with α_{1S} but at a substantially reduced proportion of only 17.7±4.8% of myotubes with α_{1S} clusters (Fig. 4C; supplementary material Fig. S3H). As expected the affinity-reducing mutation M293A diminish the ability of this β subunit to compete with endogenous β_{1a} for association with the channel complex. Conversely, within the clusters β_{1a}M293A-GFP had a dramatically increased fluorescence recovery. The fractional recovery of β_{1a}M293A-GFP was 3-fold higher (R_{75}, 45.2±3.9%) than that of wild type β_{1a}-GFP (Fig. 4F,G). This indicates that a mutation in the α binding pocket known to reduce the affinity of β_{1a}–α_{1S} binding decreases the stability of the α_1–β complex and increases the dynamic exchange of the mutated skeletal muscle β subunit to values similar to those of the non-skeletal muscle β isoforms.

Discussion

Here we used FRAP analysis of Ca^{2+} channel subunits expressed in dysgenic myotubes to study for the first time the dynamics of Ca_V α_1 and β subunits in the native environment of a functional Ca^{2+} signaling complex. First, the relative dynamics of α_1 and β subunits revealed that β_{1a} forms a stable complex with Ca_V1 α_1 subunits, whereas β_{2a}, β_{4b} and a β_{1a} mutant (M293A) form dynamic complexes with these L-type Ca^{2+} channels. Secondly, our data suggest that the specific strengths of β association with the Ca^{2+} channel complex are intrinsic properties of the β subunits, regardless to whether they form homologous or heterologous pairs with the α_1 subunit and likely independent of skeletal muscle-specific interactions with the RyR1.

Different β isoforms can form either stable or dynamic complexes with the α_1 subunits

The question as to whether auxiliary β subunits can dynamically exchange with functional Ca^{2+} channels in the membrane has been highly controversial. High affinity binding of all β isoforms with the AID in the I–II loop of high-voltage-activated Ca^{2+} channels (De Waard et al., 1995; Van Petegem et al., 2008) indicates that α_1 and β subunit form essentially irreversible complexes. However, emerging experimental evidence from heterologous expression systems suggests that in cells the α_1–β interaction might be reversible (Buraei and Yang, 2010). Injection of β subunits into *Xenopus* oocytes expressing α_1 subunits alone or in combination with another β isoform rapidly altered the gating properties of the Ca^{2+} currents (Hidalgo et al., 2006; Yamaguchi et al., 1998). Perfusion of skeletal muscle membrane vesicles with purified β_{1a} doubled current densities but not ON gating charges within 15 minutes (García et al., 2002). Injection of competing AID peptide into HEK cells transfected with $Ca_V1.2$ and β_{2a} inhibited β modulation of the single channel properties within a few minutes (Hohaus et al., 2000); and HEK cells cotransfected with $Ca_V1.2$ plus different ratios of β_{1a} and β_{2b} showed mode shifting in single channel recordings, consistent with the sequential association of distinct β subunits with the channel on a minute time scale (Jangsangthong et al., 2011). Whereas these and similar studies reviewed in (Buraei and Yang, 2010) indicate that in *Xenopus* oocytes and mammalian cells the α_1–β interaction indeed can be reversed, the question as to whether this occurs in native Ca^{2+} channel signaling complexes remained hitherto unanswered.

Our FRAP analysis addresses this problem in one of the best characterized Ca^{2+} channel signaling complexes, the skeletal muscle triad. Unexpectedly, the results give a differentiated answer to this question. On the one hand, the homologous skeletal muscle β_{1a} isoform forms stable complexes with Ca_V1 channels. Both the $Ca_V1.1$ α_{1S} subunit and the β_{1a} subunit have similarly low recovery rates, indicating that the two subunits remain stably associated to each other for the entire life time of the channel in the signaling complex. Although it has never before been demonstrated, the fact that homologous Ca^{2+} channel subunit pairs form stable complexes in its native environment may not appear surprising. But note that the skeletal muscle β_{1a} subunit formed similarly stable complexes with the non-skeletal muscle $Ca_V1.2$ α_{1C} subunit. On the other hand, the non-skeletal muscle β_{2a} and β_{4b} isoforms formed dynamic complexes with Ca_V1 channels in the junctions. Two to three times higher FRAP rates of β_{2a}-eGFP and β_{4b}-eGFP compared with the α_1 subunit unambiguously demonstrate that these β isoforms can dynamically exchange with the α_1 subunits in the triadic signaling complex on a minute time scale. Interestingly, dynamic interactions were not limited to heterologous α_1–β pairs, but were also observed for β_{2a} with its native partner $Ca_V1.2$. While such a differential ability to form stable or dynamic subunit complexes would not have been predicted from previous biochemical analysis of α_1–β interactions, functionally it appears reasonable. Skeletal muscle expresses only one set of Ca^{2+} channel subunits and β_{1a} serves primarily structural functions like the organization of tetrads (Schredelseker et al., 2005). Consequently there is no need for dynamic exchange. In contrast, neurons express multiple α_1 and β isoforms including β_{2a} and β_{4b}, which confer distinct gating properties to the channels. Consequently, dynamic exchange of β subunits with α_1 subunits expressed in the membrane provides a mechanism for current modulation. Recently we found very similar low FRAP recovery rates of α_{1C} Ca^{2+} channels in somatodendritic Ca^{2+} channel clusters in hippocampal neurons (Di Biase et al., 2011). Apparently, voltage-gated Ca^{2+} channels are stably incorporated in signaling complexes of muscle and nerve cells. Whether β_{2a} and β_{4b} subunits also show dynamic exchange in these neuronal Ca^{2+} channel complexes remains to be shown.

The differential stability of β subunits in Ca^{2+} channel complexes is an intrinsic property of the β subunits

The observed differences in FRAP rates of β subunits could result from different affinity binding of the AID to the α binding pocket, by secondary binding sites between the two channel subunits, or by interactions with other binding proteins in the triad, foremost the RyR1. The molecular organization of the $Ca_V1.1$ channel in skeletal muscle triads and peripheral couplings is unique. It is arranged in tetrad arrays corresponding in size and orientation to the underlying RyR1s with which $Ca_V1.1$ physically interacts in the process of skeletal muscle EC-coupling (Franzini-Armstrong et al., 1998). The β_{1a} subunit is essential for the organization of this functional assembly (Schredelseker et al., 2005). Therefore it is reasonable to assume that the same protein–protein interactions contribute to the stable anchoring of the Ca^{2+} channel subunits in the junctions. However, the stability of β_{1a}-GFP did not decrease when it was coexpressed with the cardiac/neuronal $Ca_V1.2$, which does not form tetrads opposite the RyR1. Furthermore, introducing mutations into $Ca_V1.1$ expected to rotate the β_{1a} subunit relative to the α_1 subunit (Mitra-Ganguli et al., 2009; Vitko et al., 2008) and probably also in relation to the RyR1 did not reduce the stability of β_{1a}

association with the complex. Together these observations indicate that the stability of β_{1a} in the triads and its role in tetrad formation are independent of its putative direct interactions with the RyR1, unless such interactions would be highly conformationally flexible. The conclusion that binding to the RyR1 does not substantially contribute to the immobilization of β_{1a} in the triad is consistent with our previous observation that β_{1a}-GFP expressed without an α_1 subunit is not targeted into the junctional clusters (Neuhuber et al., 1998a), and is further substantiated by our present FRAP data, showing that β_{1a}-GFP expressed alone recovered at the rate of free eGFP, indicating that it is freely diffusible in the cytoplasm. Thus, its stable anchoring in the triad junctions entirely depends on the coexpression of an α_1 subunit and the strength of α_1–β interactions in the context of skeletal muscle Ca^{2+} release units is the same for the homologous $Ca_V1.1$ and the heterologous $Ca_V1.2$ isoform.

The latter also indicates that the different strengths of α_1–β complexes are independent of isoform-specific differences in the α_1 subunit I–II loop sequences. The FRAP rates of β_{1a} were equally low when expressed with $Ca_V1.1$, $Ca_V1.2$ and even α_{1S}I–IIA carrying the I–II loop of $Ca_V2.1$. Conversely, the FRAP rates of β_{2a} and β_{4b} were always high regardless of the coexpressed α_1 construct. This is consistent with biochemical studies in which similar affinities of β_{2a} to the AID of $Ca_V1.1$ and $Ca_V1.2$ were measured (Van Petegem et al., 2008). Apparently, differences in the non-conserved residues of the AID and in the flanking sequences of the I–II loop do not explain the different strength of association of β_{1a} versus β_{2a} and β_{4b}. Consequently, the differences appear to be intrinsic properties of the β subunits. This interpretation is substantiated by our experiment in which we mutated the α binding pocket of β_{1a} subunit in position M293. Analogous mutations in β_{2a} have previously been shown to reduce the affinity of binding to AID and expressed channels (Maltez et al., 2005; Opatowsky et al., 2004; Van Petegem et al., 2008). In our study the M293A substitution caused a threefold increase of the fluorescence recovery rate of β_{1a}. This result provides a proof of principle for the suitability of our FRAP analysis to detect differences in α_1–β affinity and it demonstrates that the α binding pocket, and thus the interaction with the AID, are crucial for the immobilization of β_{1a} to the triadic Ca^{2+} channel complex. Nevertheless, it is important to note that the mutated methionine and other key residues of the α binding pocket are conserved between β_{1a}, β_{2a} and β_{4b}, and therefore the intrinsic differences in their ability to form stable and dynamic complexes, respectively, must be determined by non-conserved residues affecting directly or indirectly the affinity of the α binding pocket or secondary interactions with the α_1 subunit. As the modulatory functions of β subunits are highly sensitive to mutations in all domains of β (for a review, see Buraei and Yang, 2010), also the molecular mechanism resulting in more or less stable associations of β with the channel complex may arise from allosteric effects on the tertiary structure of β by non-conserved sequences anywhere in the protein.

In conclusion, determining the relative dynamics of Ca^{2+} channel α_1 and β subunits using FRAP analysis represents a new approach to study protein–protein interactions of macromolecular signaling complexes live and *in situ*, and here it provided the first direct evidence for the dynamic exchange of β subunits within a functional Ca^{2+} channel complex.

Materials and Methods

Cell culture and transfection

Myotubes of the homozygous dysgenic (mdg/mdg) cell line GLT were cultured as previously described (Powell et al., 1996). At the onset of myoblast fusion, GLT cell cultures were transfected with plasmids coding for the Ca^{2+} channel subunits using FuGeneHD transfection reagent (Roche Diagnostics) according to the manufacturer's instructions. A total of 2 μg of plasmid DNA was used per 60 mm culture dish.

Plasmids and cloning procedures

For the expression plasmids, see Table 1. *pβA-β_{2a}-eGFP*. Rat β_{2a} (GenBank number M80545) was isolated from pβA-β_{2a}-V5 (Obermair et al., 2010) by *Hin*dIII/*Bgl*II digest and cloned in the respective sites of pβA-β_{4b}-eGFP. *pc-a1SI–IIa*. Part of the α_{1S} channel with the I–II loop of α_{1A} was isolated from GFP-α_{1S}Sk-I–IIa (Flucher et al., 2000b) by SfiI/Bsu36I digest and cloned into the respective sites of pc-α_{1S}. *pc-α_{1S}del1(Δ344)*, *pc-α_{1S}del2(Δ344–345)*, *pc-α_{1S}del3(Δ344–346)*. The deletions of amino acid 344, 344–345, and 344–345–346 of α_{1S} were introduced by SOE-PCR. Briefly for each construct, the I–II loop cDNA sequence of α_{1S} was PCR amplified with overlapping mutagenesis primers in separate PCR reactions using pc-α_{1S} as template. The two separate PCR products were then used as templates for a final PCR reaction with flanking primers to connect the nucleotide sequences. This fragment was then SfiI/Bsu36I digested and cloned into the respective sites of pc-α_{1S}. *pcDNA3-β_{1a}M293A-GFP*. The mutation in position 293 was introduced by SOE-PCR. Briefly, the cDNA sequence of β_{1a} was PCR amplified with overlapping mutagenesis primers in separate PCR reactions using pcDNA3-β_{1a}-GFP as template. The two separate PCR products were then used as templates for a final PCR reaction with flanking primers to connect the nucleotide sequences. This fragment was then SacI/*Bam*HI digested and cloned into the respective sites of pcDNA3-β_{1a}-GFP.

FRAP experiments and data analysis

FRAP was performed on 9 days old transfected GLT myotubes using a SP-5 confocal microscope (Leica Microsystems) equipped with a 63×, 1.4 NA water-immersion lens at 37°C in an incubation chamber (EMBLEM). Cells growing on coverslips were mounted in a Ludin chamber in Tyrode's physiological solution containing (in mM): 130 NaCl, 2.5 KCl, 2 $CaCl_2$, 2 $MgCl_2$, 10 HEPES, 30 glucose. For all recordings myotubes with low to medium GFP fluorescence were selected to exclude overexpressing cells. Fluorescence was excited using the 488 nm line of the argon laser and recorded at a bandwidth of 500–550 nm. For GFP-α_{1S} and GFP-α_{1C}, images were acquired at 1.33 Hz in the pre-bleach, bleach and post-bleach phase (respectively 10, 6 and 100 frames) and for extended observation, an additional 30 and 40 frames were acquired at a 3 and 5 s interval, respectively. For all other experiments, images were acquired at 0.67 Hz in the pre-bleach, bleach and post-bleach phase (respectively 10, 3 and 50 frames). For extended observation, an additional 54 frames were acquired at a 5 s interval. For imaging in the pre-bleach and post-bleach phases the laser was set to 15–20% of the initially adjusted laser power (70%). A circular 6 μm diameter ROI was photobleached by scanning with the 488 nm line of argon laser at 100% intensity. Inside the bleached region, three 1.4 μm diameter ROIs were placed over clusters

and three in the cluster-free regions in between. The average fluorescence of the cluster-free regions was set as background. The average fluorescence of the three ROIs on the clusters was background subtracted and corrected for the overall bleaching in each time frame. Then the average fluorescence of the clusters was normalized so that the pre-bleach intensity was set to 1 and the first frame after photobleaching to 0 and plotted as function of time (except for cytosolic β_{1a}-GFP, β_{4b}-eGFP and eGFP, where only the pre-bleach intensity was set to 1). The analysis of fluorescence was performed using LAS AF software (Leica Microsystems). Recovery curves were fitted with a straight line or a monoexponential fit with pClamp software (version 8.0, Molecular Devices) and the value of the fitted curve at 75 s after bleaching was chosen to calculate the mean rate of fluorescence recovery (R_{75}). Results are expressed as mean±s.e. All data were organized in MS Excel and analyzed using ANOVA with Tukey post-hoc analysis in SPSS statistical software (SPSS Inc., Chicago IL, USA). Correlation analysis of the average fluorescence intensity of myotubes, as well as the average size and fluorescence intensity of the clusters with the corresponding FRAP (R_{75}) values recorded in the same cell did not reveal any correlation between any of these parameters (supplementary material Fig. S6). This indicated that the variability of expression levels or differences in the subcellular distribution of the constructs cannot account for the observed differences of FRAP values.

Triad targeting and β co-clustering quantification

Paraformaldehyde-fixed cultures were double-immunolabeled [as previously described in (Flucher et al., 2000b)] with the monoclonal α_{1S} antibody mAb 1A (1:4000) (Kugler et al., 2004) and the rabbit anti-GFP (serum, 1:10,000; Molecular Probes, Eugene, OR) and fluorescence-labeled with Alexa-594- and Alexa-488-conjugated secondary antibody, respectively. Thus, the anti-GFP label and the intrinsic GFP signal were both recorded in the green channel. Triad targeting of the α_{1S} chimera and mutants was quantified by systematically screening the coverslips for transfected myotubes using a 63×, 1.4 NA objective Axioimager microscope (Carl Zeiss, Inc.). The labeling patterns of transfected myotubes with more than four nuclei were classified as either ‘clustered’ or ‘not clustered’. Quantitative analysis of β co-clustering was performed by systematically screening for clustered myotubes in the red channel (same criteria described for the triad targeting) and classifying them as β co-clustered or not in the green channel. The counts were obtained from samples of three separate experiments. For RyR staining, in GFP-α_{1S} and GFP-α_{1C} transfected cells, samples were double-immunolabeled with the rabbit anti-GFP (serum, 1:10,000) and mouse monoclonal anti RyR (34-C, 1:1000, Alexis Biochemicals, Lausen, Switzerland), and fluorescence-labeled with Alexa-594- and Alexa-488-conjugated secondary antibody, respectively. In untagged α_{1S} expressing cells, samples were double-immunolabeled with the monoclonal α_{1S} antibody mAb 1A (1:4000) and rabbit anti RyR1 [1:2000; (Flucher et al., 1999)] and fluorescence-labeled with Alexa-594- and Alexa-488-conjugated secondary antibody, respectively. 14-bit images were recorded with cooled CCD cameras (SPOT; Diagnostic Instruments, Stirling Heights, MI, USA) and Metaview image processing software (Universal Imaging, Corp., West Chester, PA, USA).

Image processing

Image composites were arranged in Adobe Photoshop CS3 (Adobe Systems Inc.) and, where necessary, linear adjustments were performed to correct black level and contrast.

Supplementary Material

Refer to Web version on PubMed Central for supplementary material.

Acknowledgments

We thank Ariane Benedetti and Roman Egger for excellent technical assistance, Bruno Benedetti for electrophysiology, Gerald Obermair for help with statistical analysis, Martin Offterdinger of the Biooptics Facility for assistance at the confocal microscope and Benedikt Nimmervoll for software assistance.

Funding: This study was supported by the Austrian Science Fund (FWF) [grant numbers P23479-B19 and W01101 to B.E.F. and T443-B18 to V.D.B.].

References

Buraei Z, Yang J. The β subunit of voltage-gated Ca2+ channels. Physiol. Rev. 2010; 90:1461–1506. [PubMed: 20959621]

Cheng W, Altafaj X, Ronjat M, Coronado R. Interaction between the dihydropyridine receptor Ca2+ channel beta-subunit and ryanodine receptor type 1 strengthens excitation-contraction coupling. Proc. Natl. Acad. Sci. USA. 2005; 102:19225–19230. [PubMed: 16357209]

Chien AJ, Carr KM, Shirokov RE, Rios E, Hosey MM. Identification of palmitoylation sites within the L-type calcium channel beta2a subunit and effects on channel function. J. Biol. Chem. 1996; 271:26465–26468. [PubMed: 8900112]

De Waard M, Witcher DR, Pragnell M, Liu H, Campbell KP. Properties of the alpha 1-beta anchoring site in voltage-dependent Ca2+ channels. J. Biol. Chem. 1995; 270:12056–12064. [PubMed: 7744854]

Di Biase V, Tuluc P, Campiglio M, Obermair GJ, Heine M, Flucher BE. Surface traffic of dendritic CaV1.2 calcium channels in hippocampal neurons. J. Neurosci. 2011; 31:13682–13694. [PubMed: 21940459]

Flucher BE, Conti A, Takeshima H, Sorrentino V. Type 3 and type 1 ryanodine receptors are localized in triads of the same mammalian skeletal muscle fibers. J. Cell Biol. 1999; 146:621–630. [PubMed: 10444070]

Flucher BE, Kasielke N, Gerster U, Neuhuber B, Grabner M. Insertion of the full-length calcium channel alpha(1S) subunit into triads of skeletal muscle in vitro. FEBS Lett. 2000a; 474:93–98. [PubMed: 10828458]

Flucher BE, Kasielke N, Grabner M. The triad targeting signal of the skeletal muscle calcium channel is localized in the COOH terminus of the alpha(1S) subunit. J. Cell Biol. 2000b; 151:467–478. [PubMed: 11038191]

Franzini-Armstrong C, Protasi F, Ramesh V. Comparative ultrastructure of Ca2+ release units in skeletal and cardiac muscle. Ann. N. Y. Acad. Sci. 1998; 853:20–30. [PubMed: 10603933]

García R, Carrillo E, Rebolledo S, García MC, Sánchez JA. The beta1a subunit regulates the functional properties of adult frog and mouse L-type Ca2+ channels of skeletal muscle. J. Physiol. 2002; 545:407–419. [PubMed: 12456821]

Grabner M, Dirksen RT, Beam KG. Tagging with green fluorescent protein reveals a distinct subcellular distribution of L-type and non-L-type Ca2+ channels expressed in dysgenic myotubes. Proc. Natl. Acad. Sci. USA. 1998; 95:1903–1908. [PubMed: 9465115]

Grabner M, Dirksen RT, Suda N, Beam KG. The II-III loop of the skeletal muscle dihydropyridine receptor is responsible for the Bi-directional coupling with the ryanodine receptor. J. Biol. Chem. 1999; 274:21913–21919. [PubMed: 10419512]

Hidalgo P, Gonzalez-Gutierrez G, Garcia-Olivares J, Neely A. The alpha1-beta-subunit interaction that modulates calcium channel activity is reversible and requires a competent alpha-interaction domain. J. Biol. Chem. 2006; 281:24104–24110. [PubMed: 16793763]

Hohaus A, Poteser M, Romanin C, Klugbauer N, Hofmann F, Morano I, Haase H, Groschner K. Modulation of the smooth-muscle L-type Ca2+ channel alpha1 subunit (alpha1C-b) by the beta2a subunit: a peptide which inhibits binding of beta to the I-II linker of alpha1 induces functional uncoupling. Biochem. J. 2000; 348:657–665. [PubMed: 10839999]

Jangsangthong W, Kuzmenkina E, Böhnke AK, Herzig S. Single-channel monitoring of reversible L-type Ca(2+) channel Ca(V)α(1)-Ca(V)β subunit interaction. Biophys. J. 2011; 101:2661–2670. [PubMed: 22261054]

Kasielke N, Obermair GJ, Kugler G, Grabner M, Flucher BE. Cardiac-type EC-coupling in dysgenic myotubes restored with Ca2+ channel subunit isoforms alpha1C and alpha1D does not correlate with current density. Biophys. J. 2003; 84:3816–3828. [PubMed: 12770887]

Kugler G, Grabner M, Platzer J, Striessnig J, Flucher BE. The monoclonal antibody mAB 1A binds to the excitation--contraction coupling domain in the II-III loop of the skeletal muscle calcium channel alpha(1S) subunit. Arch. Biochem. Biophys. 2004; 427:91–100. [PubMed: 15178491]

Maltez JM, Nunziato DA, Kim J, Pitt GS. Essential Ca(V)beta modulatory properties are AID-independent. Nat. Struct. Mol. Biol. 2005; 12:372–377. [PubMed: 15750602]

Mitra-Ganguli T, Vitko I, Perez-Reyes E, Rittenhouse AR. Orientation of palmitoylated CaVbeta2a relative to CaV2.2 is critical for slow pathway modulation of N-type Ca2+ current by tachykinin receptor activation. J. Gen. Physiol. 2009; 134:385–396. [PubMed: 19858358]

Moriyoshi K, Richards LJ, Akazawa C, O'Leary DD, Nakanishi S. Labeling neural cells using adenoviral gene transfer of membrane-targeted GFP. Neuron. 1996; 16:255–260. [PubMed: 8789941]

Neuhuber B, Gerster U, Döring F, Glossmann H, Tanabe T, Flucher BE. Association of calcium channel alpha1S and beta1a subunits is required for the targeting of beta1a but not of alpha1S into skeletal muscle triads. Proc. Natl. Acad. Sci. USA. 1998a; 95:5015–5020. [PubMed: 9560220]

Neuhuber B, Gerster U, Mitterdorfer J, Glossmann H, Flucher BE. Differential effects of Ca2+ channel beta1a and beta2a subunits on complex formation with alpha1S and on current expression in tsA201 cells. J. Biol. Chem. 1998b; 273:9110–9118. [PubMed: 9535900]

Obermair GJ, Szabo Z, Bourinet E, Flucher BE. Differential targeting of the L-type Ca2+ channel alpha 1C (CaV1.2) to synaptic and extrasynaptic compartments in hippocampal neurons. Eur. J. Neurosci. 2004; 19:2109–2122. [PubMed: 15090038]

Obermair GJ, Kugler G, Baumgartner S, Tuluc P, Grabner M, Flucher BE. The Ca2+ channel alpha2delta-1 subunit determines Ca2+ current kinetics in skeletal muscle but not targeting of alpha1S or excitation-contraction coupling. J. Biol. Chem. 2005; 280:2229–2237. [PubMed: 15536090]

Obermair GJ, Schlick B, Di Biase V, Subramanyam P, Gebhart M, Baumgartner S, Flucher BE. Reciprocal interactions regulate targeting of calcium channel beta subunits and membrane expression of alpha1 subunits in cultured hippocampal neurons. J. Biol. Chem. 2010; 285:5776–5791. [PubMed: 19996312]

Opatowsky Y, Chen CC, Campbell KP, Hirsch JA. Structural analysis of the voltage-dependent calcium channel beta subunit functional core and its complex with the alpha 1 interaction domain. Neuron. 2004; 42:387–399. [PubMed: 15134636]

Powell JA, Petherbridge L, Flucher BE. Formation of triads without the dihydropyridine receptor alpha subunits in cell lines from dysgenic skeletal muscle. J. Cell Biol. 1996; 134:375–387. [PubMed: 8707823]

Schredelseker J, Di Biase V, Obermair GJ, Felder ET, Flucher BE, Franzini-Armstrong C, Grabner M. The beta 1a subunit is essential for the assembly of dihydropyridine-receptor arrays in skeletal muscle. Proc. Natl. Acad. Sci. USA. 2005; 102:17219–17224. [PubMed: 16286639]

Subramanyam P, Obermair GJ, Baumgartner S, Gebhart M, Striessnig J, Kaufmann WA, Geley S, Flucher BE. Activity and calcium regulate nuclear targeting of the calcium channel beta4b subunit in nerve and muscle cells. Channels. 2009; 3:343–355. [PubMed: 19755859]

Takekura H, Paolini C, Franzini-Armstrong C, Kugler G, Grabner M, Flucher BE. Differential contribution of skeletal and cardiac II-III loop sequences to the assembly of dihydropyridine-receptor arrays in skeletal muscle. Mol. Biol. Cell. 2004; 15:5408–5419. [PubMed: 15385628]

Tuluc P, Kern G, Obermair GJ, Flucher BE. Computer modeling of siRNA knockdown effects indicates an essential role of the Ca2+ channel alpha2delta-1 subunit in cardiac excitation-contraction coupling. Proc. Natl. Acad. Sci. USA. 2007; 104:11091–11096. [PubMed: 17563358]

Van Petegem F, Clark KA, Chatelain FC, Minor DL Jr. Structure of a complex between a voltage-gated calcium channel beta-subunit and an alpha-subunit domain. Nature. 2004; 429:671–675. [PubMed: 15141227]

Van Petegem F, Duderstadt KE, Clark KA, Wang M, Minor DL Jr. Alanine-scanning mutagenesis defines a conserved energetic hotspot in the CaValpha1 AID-CaVbeta interaction site that is critical for channel modulation. Structure. 2008; 16:280–294. [PubMed: 18275819]

Vitko I, Shcheglovitov A, Baumgart JP, Arias-Olguín II, Murbartián J, Arias JM, Perez-Reyes E. Orientation of the calcium channel beta relative to the alpha(1)2.2 subunit is critical for its regulation of channel activity. PLoS ONE. 2008; 3:e3560. [PubMed: 18958281]

Yamaguchi H, Hara M, Strobeck M, Fukasawa K, Schwartz A, Varadi G. Multiple modulation pathways of calcium channel activity by a beta subunit. Direct evidence of beta subunit participation in membrane trafficking of the alpha1C subunit. J. Biol. Chem. 1998; 273:19348–19356. [PubMed: 9668125]

Europe PMC Funders Author Manuscripts

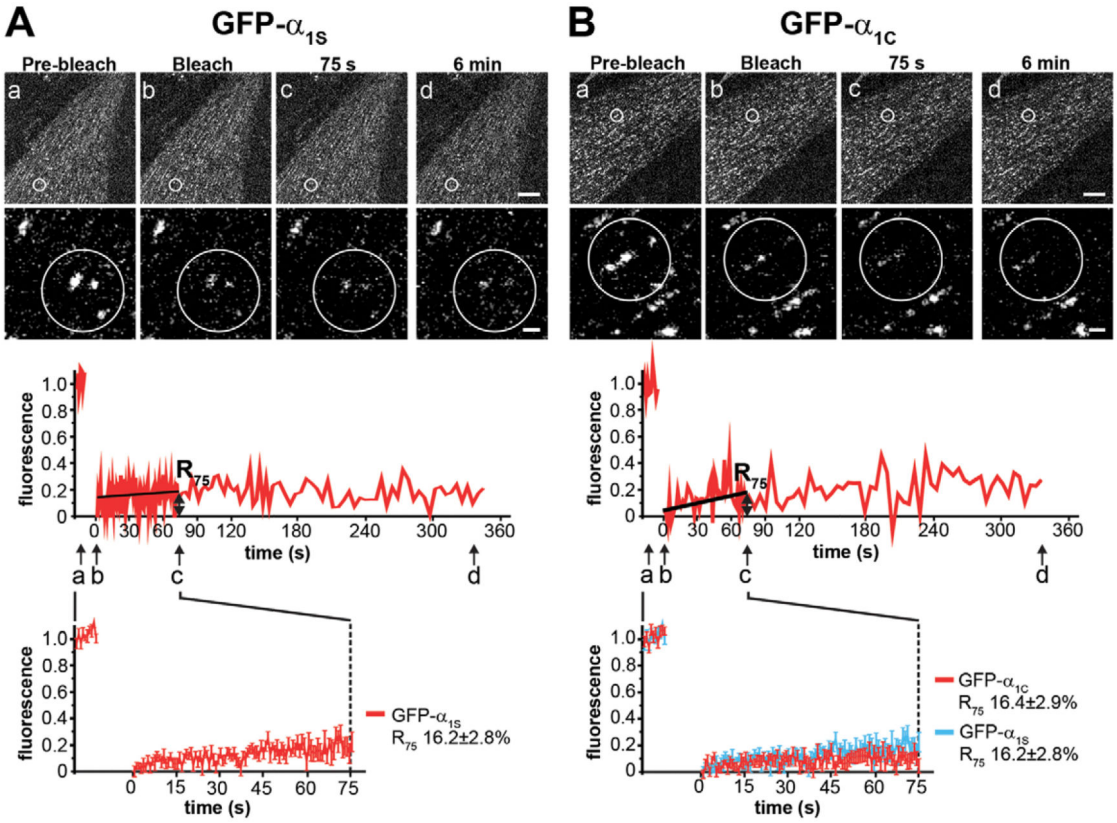

Fig. 1. FRAP analysis of GFP-α1S and GFP-α1C in skeletal muscle triad junctions

Clusters of GFP-α_{1S} (**A**) or GFP-α_{1C} (**B**) in live dysgenic myotubes were photo-bleached (within circles) and imaged for up to 6 min. Representative high-magnification images and the corresponding normalized FRAP recordings show little fluorescence recovery of the Ca^{2+} channel α_1 subunits (a–d, time points of example images). Average recovery curves [lower panels; mean±s.e., *N*=3, *n*(GFP-α_{1S})=16, *n*(GFP-α_{1C})=18] reveal a similarly low recovery of GFP-α_{1S} and GFP-α_{1C} and indistinguishable recovery rates 75 s after bleaching (R_{75}). Upper scale bar: 10 μm. Lower scale bar: 1 μm.

Europe PMC Funders Author Manuscripts

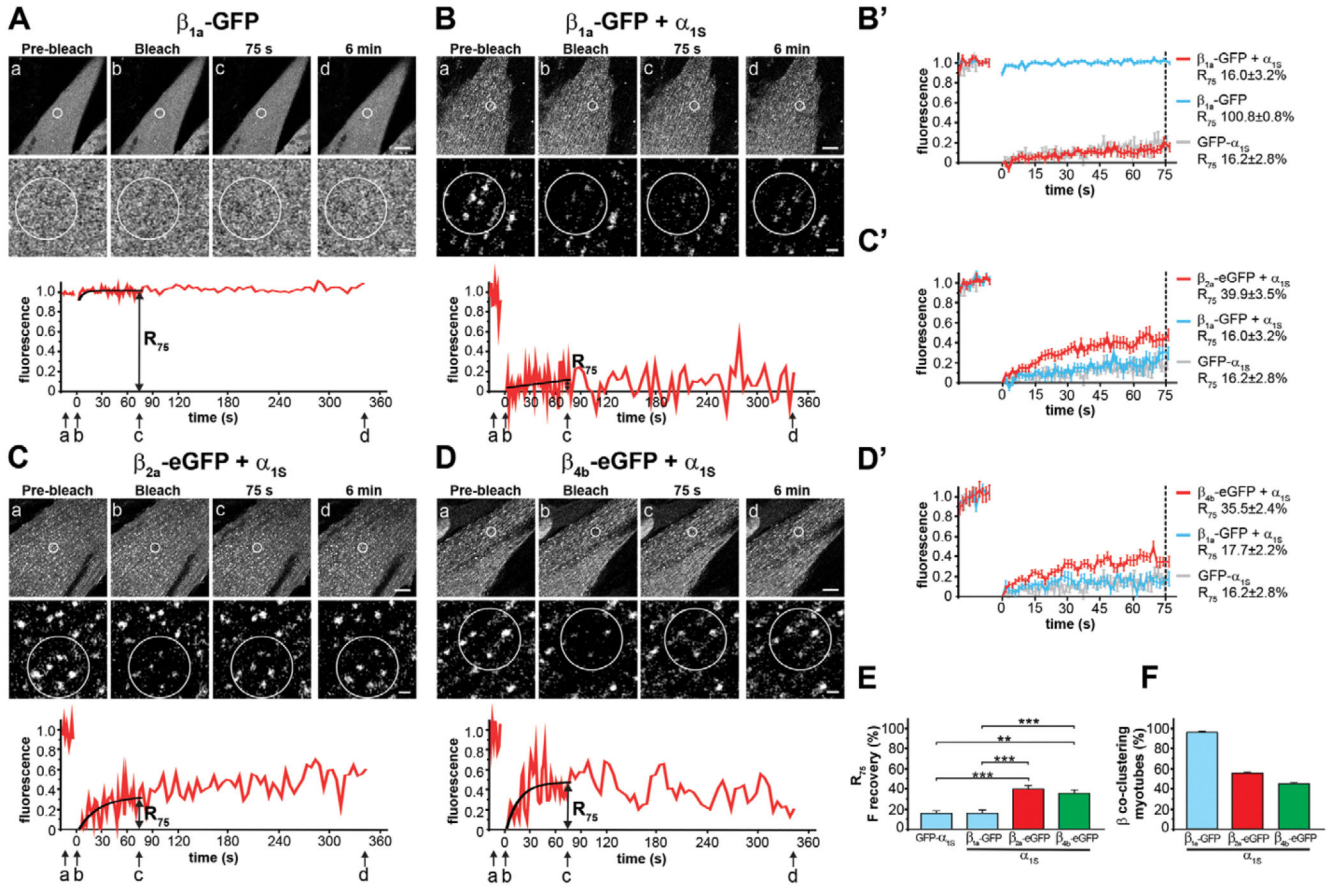

Fig. 2. FRAP analysis of β_{1a}-GFP, β_{2a}-eGFP, and β_{4b}-eGFP with and without $Ca_V1.1$ α_{1S}

(**A**) β_{1a}-GFP expressed without an α_1 subunit in dysgenic myotubes is diffusely distributed and its fluorescence recovers instantaneously after photobleaching (mean±s.e., *N*=3, *n*=3). (**B**) Coexpressed with α_{1S}, β_{1a}-GFP is localized in clusters and does not recover within 6 min after bleaching. (**B′**) Average recovery curves (mean±s.e., *N*=5, *n*=19) and R_{75} of β_{1a}-GFP reveal a high mobility when expressed alone (blue), but low mobility when coexpressed with α_{1S} (red) similar to that of GFP-α_{1S} (gray; from Fig. 1A). In contrast, β_{2a}-eGFP (**C**) and β_{4b}-eGFP (**D**) coexpressed with α_{1S} show substantial fluorescence recovery. When coexpressed with α_{1S}, mean recovery of β_{2a}-eGFP (**C′**, red) and β_{4b}-eGFP (**D′**, red) is approximately twofold higher than that of β_{1a}-GFP+α_{1S} (blue; from Fig. 2B for β_{2a}, in parallel for β_{4b}) or GFP-α_{1S} (gray; from Fig. 1A). (**E**) R_{75} (mean±s.e.) of β_{2a}-GFP (*N*=7, *n*=23) and β_{4b}-eGFP (*N*=3, *n*=17) are significantly higher compared with β_{1a}-GFP+α_{1S} or GFP-α_{1S}. Anova F(11,264)=15,6; *P*<0.001 (*P* values in the figure are for post-hoc analysis; ***P*<0.01, ****P*<0.001). (**F**) Co-localization with α_{1S} is seen in 96.6±1.9% of myotubes expressing β_{1a}-GFP, but only in 56.6±1.9% expressing β_{2a}-eGFP and 44.4±2.9% expressing β_{4b}-eGFP (*N*=3, *n*=90). Upper scale bar: 10 μm. Lower scale bar: 1 μm.

Europe PMC Funders Author Manuscripts

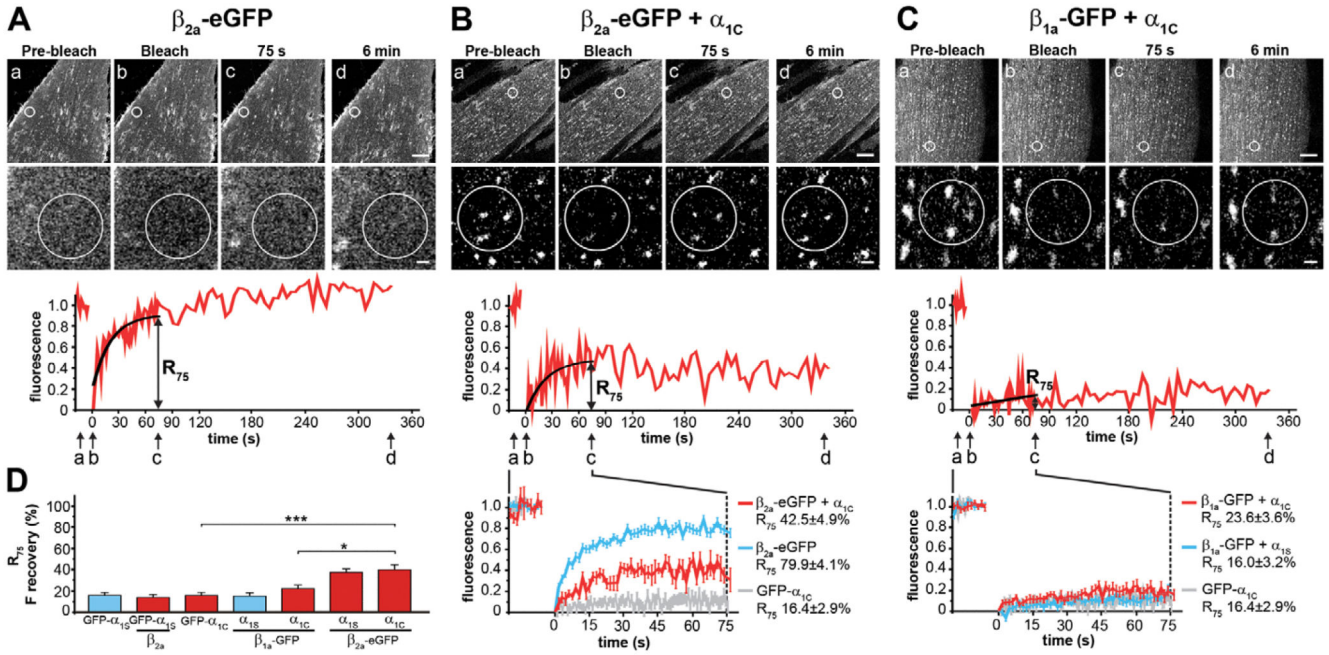

Fig. 3. FRAP analysis of β_{2a}-eGFP and β_{1a}-GFP with and without $Ca_V1.2$ α_{1C}

(**A**) The palmitoylated β_{2a}-eGFP expressed without an α_1 subunit in dysgenic myotubes is localized in the plasma membrane and its fluorescence fully recovers within 6 min after bleaching (mean recovery trace and R_{75} shown in B, blue, *N*=2 *n*=12). (**B**) When coexpressed with α_{1C}, β_{2a}-eGFP is recruited into junctional clusters and its average fluorescence recovery is significantly reduced (red), but not to the low rate of GFP-α_{1C} (gray, from Fig. 1B, *N*=4, *n*=11). (**C**) In contrast, when β_{1a}-GFP is coexpressed with α_{1C}, it shows little recovery after bleaching (red), very similar to when β_{1a}-GFP was coexpressed with α_{1S} (in parallel *N*=3, *n*=18). (**D**) Comparison of R_{75} values shows that β_{2a}-eGFP has approximately twofold higher recovery rates than β_{1a}-GFP when coexpressed with α_{1S} or α_{1C}, but coexpression of β_{2a} does not affect the recovery rate of GFP-α_{1S} (mean±s.e.). Anova F(11,264)=15,6; *P*<0.001 (*P* values in the figure are for post-hoc analysis; **P*<0.05, ****P*<0.001). Upper scale bar: 10 μm. Lower scale bar: 1 μm.

Europe PMC Funders Author Manuscripts

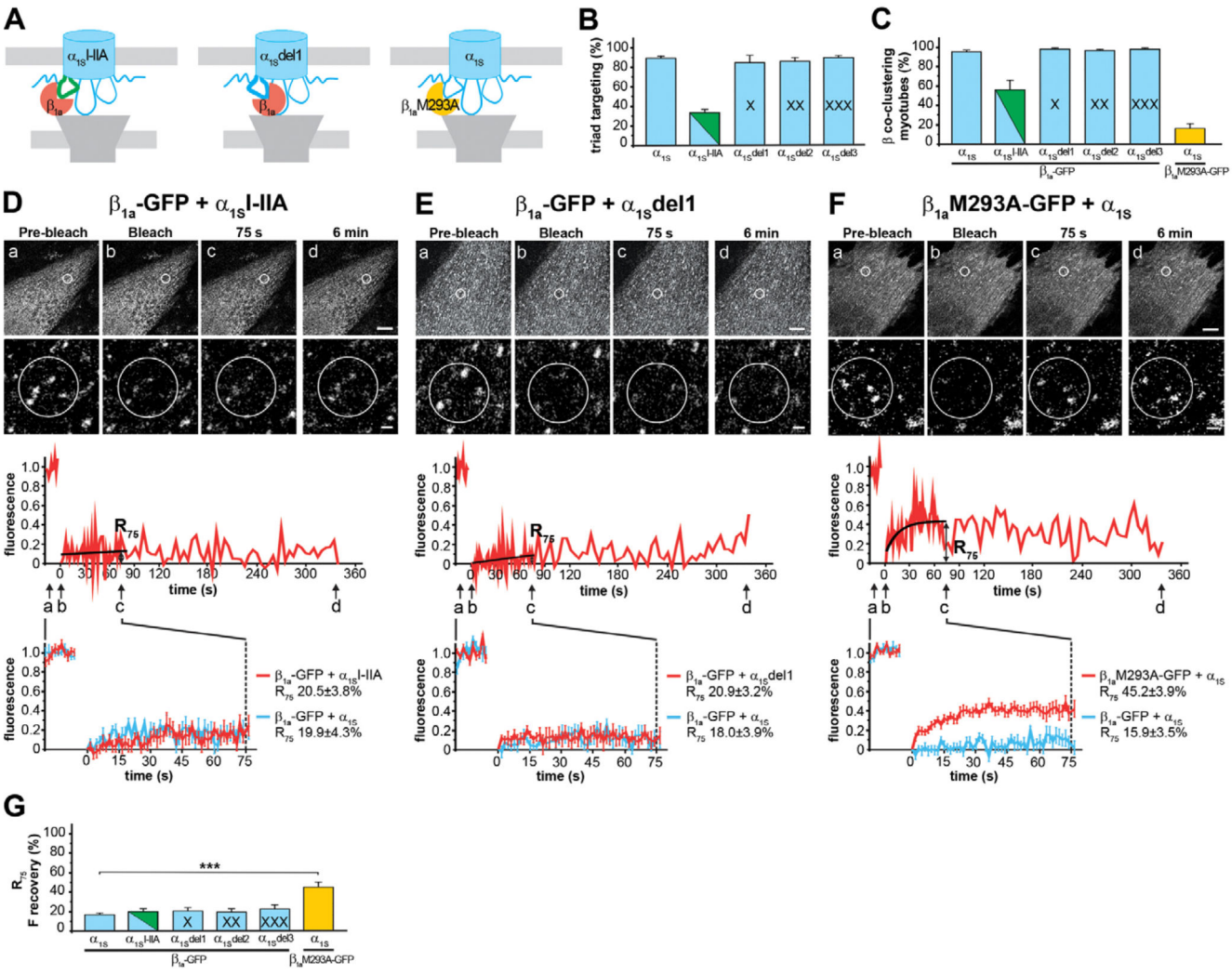

Fig. 4. Effects of mutations of the α_{1S}I–II loop and the β_{1a} subunit on co-clustering and the mobility of β_{1a}-GFP

(**A**) In α_{1S}I–IIA, the I–II loop was replaced by that of α_{1A} ($Ca_V2.1$); in α_{1S}del1, one amino acid in the proximal I–II loop was deleted to alter the orientation of the β subunit relative to the channel; in β_{1a}M293A-GFP, a single methionine was mutated to alanine. (**B**) Triad targeting was normal for the α_{1S}del1 construct, but diminished to 32.6±3.0% for α_{1S}I–IIA (*N*=3, *n*=300). (**C**) β_{1a}-GFP co-clustered efficiently with the α_{1S}del1 construct, but only in 50.6±11.4% of the myotubes expressing α_{1S}I–IIA. β_{1a}M293A-GFP co-clustered only in 17.8±4.8% of the myotubes expressing α_{1S} (*N*=3, *n*=90). When coexpressed with α_{1S}I–IIA (**D**) or with α_{1S}del1 (**E**), β_{1a}-GFP fluorescence did not recover within 6 min after bleaching. With both constructs, the mean recovery curves and R_{75} (**G**) (mean±s.e.; α_{1S}I–IIA, *N*=6, *n*=7; α_{1S}del1, *N*=3, *n*=13) were similar to that of β_{1a}-GFP and the wild type α_{1S}. When coexpressed with α_{1S} (**F**), β_{1a}M293A-GFP showed substantial fluorescence recovery: an approximately threefold higher recovery rate than β_{1a}-GFP (*N*=7, *n*=25). Anova

F(11,264)=15,6; $P<0.001$ (P values in the figure are for post-hoc analysis; ***$P<0.001$). Upper scale bar: 10 μm. Lower scale bar: 1 μm.

Europe PMC Funders Author Manuscripts

Europe PMC Funders Author Manuscripts

Table 1

Expression plasmids

Plasmid	GenBank number	Promoter	Reference
GFP-α1S	NM_001101720	CMV	Grabner et al., 1998
GFP-α1C	X15539	CMV	Grabner et al., 1998
pc-α1S	NM_001101720	CMV	Neuhuber et al., 1998b
pβA-α1C	M67515	pβA	Di Biase et al., 2011
pcDNA3-β1a-GFP	M25514	CMV	Neuhuber et al., 1998b
pβA-β2a-eGFP	M80545	pβA	The present study
pβA-β2a-V5	M80545	pβA	Obermair et al., 2010
pβA-β4b-eGFP	LO2315	pβA	Subramanyam et al., 2009
pc-α1SI–IIA		CMV	Subramanyam et al., 2009
pc-α1Sdel1		CMV	The present study
pc-α1Sdel2		CMV	The present study
pc-α1Sdel3		CMV	The present study
pcDNA3-β1aM293A-GFP		CMV	The present study
pβA-eGFP		pβA	Obermair et al., 2004
GAP-GFP		pAdV	Moriyoshi et al., 1996